Journal of Cerebral Blood Flow & Metabolism (2012) 32, 33–40

www.jcbfm.com

Cerebral oxygen metabolism of rats using injectable ^{15}O-oxygen with a steady-state method

Masato Kobayashi[1,2], Tetsuya Mori[1], Yasushi Kiyono[1], Vijay Narayan Tiwari[1], Rikiya Maruyama[1], Keiichi Kawai[1,2] and Hidehiko Okazawa[1,3]

[1]*Biomedical Imaging Research Center, University of Fukui, Fukui, Japan;* [2]*School of Health Sciences, College of Medical, Pharmaceutical and Health Sciences, Kanazawa University, Ishikawa, Japan;* [3]*Research and Education Program for Life Science, University of Fukui, Fukui, Japan*

To develop a less-stressful and simple method for measurement of the cerebral metabolic rate of oxygen (*CMRO$_2$*) in small animals, the steady-state method was applied to injectable $^{15}O_2$-PET ($^{15}O_2$-positron emission tomography) using hemoglobin-containing vesicles ($^{15}O_2$-HbV). Ten normal rats and 10 with middle cerebral arterial occlusion (MCAO) were studied using a small animal PET scanner. A series of ^{15}O-PET scans with C^{15}O-labeled HbV, $H_2^{15}O$, and $^{15}O_2$-HbV were performed with 10 to 15 minutes intervals to measure cerebral blood volume (*CBV*), cerebral blood flow (*CBF*), and *CMRO$_2$*. Positron emission tomography scans were started with a tracer injection using a multiprogramming syringe pump, which provides a slowly increasing injection volume to achieve steady-state radioactivity for $H_2^{15}O$ and $^{15}O_2$-HbV scans. The radioactivity concentration of ^{15}O rapidly achieved equilibrium in the blood and whole brain at about 2 minutes after $H_2^{15}O$ and $^{15}O_2$-HbV administration, which was stable during the scans. The whole brain mean values of *CBF*, *CBV*, and *CMRO$_2$* were 54.3 ± 2.0 mL per 100 g per minute, 4.9 ± 0.4 mL/100 g, and 2.8 ± 0.2 μmoL per g per minute (6.2 ± 0.4 mL per 100 g per minute) in the normal rats, respectively. In the MCAO model rats, all hemodynamic parameters of the infarction area on the occlusion side significantly decreased. The steady-state method with ^{15}O-labeled HbV is simple and useful to analyze hemodynamic changes in studies with model animals.
Journal of Cerebral Blood Flow & Metabolism (2012) **32,** 33–40; doi:10.1038/jcbfm.2011.125; published online 24 August 2011

Keywords: ^{15}O-gas PET; cerebral oxygen metabolism; hemoglobin-containing vesicles; injectable $^{15}O_2$; steady-state method

Introduction

^{15}O-gas positron emission tomography (PET) has been used to clarify the mechanisms of cerebrovascular diseases (CVDs) using PET (Temma *et al*, 2006, 2008). An intravenous injectable $^{15}O_2$ method was proposed using a special device and the blood was collected from another rat because radioactivity of ^{15}O-gas from the airways affects measurement of cerebral radioactivity counts (Magata *et al*, 2003; Temma *et al*, 2006). Our previous study reported the feasibility of another injectable $^{15}O_2$ method using artificial hemoglobin-containing vesicles (HbV), which does not require killing of other rats for blood collection and the special device (Tiwari *et al*, 2010). Since these injectable $^{15}O_2$ methods applied bolus injection of tracers to measure cerebral hemodynamic parameters, multipoint arterial blood samplings to obtain arterial input functions were required, which may be stressful for small animals and may change physical conditions. Therefore, we developed a new steady-state method for cerebral blood flow (*CBF*) measurement using $H_2^{15}O$ and a multiprogramming syringe pump that provides a slowly increasing injection volume to reduce rats' stress (Kobayashi *et al*, 2011). The steady-state method is ideal for small animal studies because the injection volumes and blood samplings are limited.

The purpose of this study was to apply the steady-state method to $^{15}O_2$-labeled HbV ($^{15}O_2$-HbV) PET scans to measure the cerebral metabolic rate of oxygen (*CMRO$_2$*). C^{15}O-labeled HbV (C^{15}O-HbV) PET was also performed to obtain the cerebral blood volume (*CBV*), which is usually used for correction of the oxygen extraction fraction (*OEF*).

Correspondence: Professor H Okazawa, Biomedical Imaging Research Center, University of Fukui, 23-3 Matsuoka-Shimoaizuki, Eiheiji-cho, Fukui 910-1193, Japan.
E-mail: okazawa@u-fukui.ac.jp
This study was partly funded by a Grant-in-Aid for Scientific Research from Japan Society for the Promotion of Science (19790861, 22791180) and the Fukui Brain Project, Research and Education Program for Life Science, University of Fukui.
Received 29 April 2011; revised 27 July 2011; accepted 28 July 2011; published online 24 August 2011

Materials and methods

Labeling Procedure of Hemoglobin-Containing Vesicles

The synthesis and purification processes of HbV (Oxygenix Co. Ltd., Tokyo, Japan) and rheological properties of HbV were described previously in detail (Phillips *et al*, 1997; Ogata, 2000; Takeoka *et al*, 2002; Tiwari *et al*, 2010). L-cysteine (2.8 mM) was added to HbV vials, which were kept under anoxic conditions. The HbV was labeled with $C^{15}O$ and $^{15}O_2$ by the method reported previously (Tiwari *et al*, 2010). The HbV solution of 2 mL for $C^{15}O$ labeling and 8 mL for $^{15}O_2$ labeling was prepared in a 50-mL volume vial. Target gas containing $C^{15}O$ or $^{15}O_2$ was delivered into the HbV solution through a bubbling needle. The bubbling time of the radioactive gas was 2 minutes, and the vial was vortexed during $^{15}O_2$ bubbling. Labeled HbV was then sampled using a syringe and radioactivity was measured using a dose meter (Capintec Inc., Ramsey, NJ, USA).

Animal Positron Emission Tomography Studies

Animal studies were approved by the Animal Care Committee at the University of Fukui and conducted in accordance with the international standards for animal welfare and institutional guidelines. Adequate measures were taken to minimize pain and discomfort. Male Sprague-Dawley rats from Japan SLC Inc. (Hamamatsu, Japan) were housed for 1 week under a 12-hour light/12-hour dark cycle with free access to food and water. The rats were fasted with no food overnight with water supplied *ad libitum* before the PET experiments.

Twenty rats ($298.5 \pm 8.8\,g$) were anesthetized with an intraperitoneal injection of chloral hydrate (0.4 mg/g body weight, intraperitoneally). A PE-50 catheter was inserted into the femoral artery for blood sampling and the femoral vein for ^{15}O-radiotracers administration. In 10 rats, the left middle cerebral artery (MCA) was occluded intraluminally using a nylon 4-0 surgical monofilament (Ethilon; Ethicon, Inc., Somerville, NJ, USA) for 1 hour before the PET scans (Longa *et al*, 1989; Kuge *et al*, 1995). The PET studies were performed with a list-mode scan protocol using a small animal PET scanner (SHR-41000; Hamamatsu Photonics, Hamamatsu, Japan) (Yamada *et al*, 2008). The scanner acquires 213 slices covering an axial length of 160 mm, with a three-dimension mode, achieving a resolution of $\sim$2.0 mm full width at half maximum in the transaxial direction and 2.8 mm full width at half maximum in the axial direction. The rats were placed in a supine position on the scanner bed, and the limbs were fixed using surgical tape. The orientation of the cranial position was determined using a laser beam on the scanner. During the PET scan, body temperature was maintained at about 37°C using a controller (TC-1, Brainscience idea, Osaka, Japan). Before emission scans, a transmission scan was performed for attenuation correction using a $^{68}Ge/^{68}Ga$ external source. A 3-minute PET scan was started with an intravenous bolus administration of about 20 MBq $C^{15}O$-HbV in a 0.4-mL injection volume. Approximately 10 μL of arterial blood was sampled every 1 minute, and radioactivity in the blood samples was immediately measured with a well scintillation counter (ARC380; Aloka, Tokyo, Japan). After the decay of $C^{15}O$, a 5-minute scan was started with intravenous administration of $\sim$185 MBq $H_2^{15}O$. The 3-mL tracer was injected using a 10-mL syringe set up on a multiprogramming syringe pump (FP-2000; Melquest, Toyama, Japan). Details of this steady-state method were described in our previous report (Kobayashi *et al*, 2011). About 50 μL arterial blood was sampled every 1 minute during the $H_2^{15}O$ scan, and radioactivity in the blood samples was immediately measured with the well scintillation counter. After the decay of $H_2^{15}O$, a 5-minute PET data acquisition was started with intravenous administration of $\sim$185 MBq $^{15}O_2$-HbV in a 3-mL volume using the same injection method as for the $H_2^{15}O$ scan. Briefly, the injection speed was controlled rapidly for the first 5 seconds to fill the dead volume of the venous line with a small amount of overshoot, the rate was then changed moderately for 40 seconds to increase blood radioactivity, followed by a slow but gradually increasing administration rate to compensate for the decay in blood ^{15}O radioactivity. To compensate for the decay in blood ^{15}O radioactivity in the later phase, the injection rate was continuously changed under the assumption of an inverse decay function as expressed by the following equation:

$$v = 117 \cdot \exp(1.0 \times 10^{-2} \cdot \lambda \cdot t) \quad (1)$$

here v (μL/min) is the injection velocity for the syringe pump, λ (/min) is the decay constant of ^{15}O, and t (minutes) is the time after the injection of ^{15}O-radiotracers. The same constants were used in the equation for both $^{15}O_2$-HbV and $H_2^{15}O$ administration. About 200 μL arterial blood was sampled every 1 minute during the $^{15}O_2$-HbV scan. In all, 50 μL of the arterial blood was put into a microtube to measure whole blood radioactivity. In all, 50 μL acetonitrile, a deproteinization agent, was added into the remaining arterial blood and the sample was centrifuged at 3000 g for 2 minutes. About 100 μL of supernatant fluid including acetonitrile was obtained, and radioactivity was immediately measured with a well scintillation counter. Arterial blood gases and other physiological parameters were measured using a blood gas analyzer (ABL555; Radiometer, Copenhagen, Denmark) and a hemooximeter (OSM3; Radiometer) after the transmission scan, and before and after the $^{15}O_2$-HbV PET scan.

Magnetic Resonance Imaging Scan and 2,3,5-Triphenyl-Tetrazolium Chloride Staining

After PET scans, the normal rats and 3 of the 10 MCA occlusion (MCAO) model rats were scanned by magnetic resonance imaging (MRI) using a 3.0-T MRI scanner (Signa Horizon, GE Medical Systems, Milwaukee, WI, USA). In the MRI scans, the rats were placed and fixed between a pair of surface coils. T2-weighted images of each rat's brain were acquired using a fast spin echo method with repetition time/echo time of 5050/85 milliseconds, 256×256 matrix, slice thickness 1.0 mm, spacing 0 mm, field of view 10 cm, phase-field of view 8 cm and excitation number of 3. The rat brains were removed immediately after the MRI scans, sliced and stained with 2,3,5-

triphenyl-tetrazolium chloride (TTC). The remaining seven rats with MCAO were killed immediately after the PET scans, and the brains were sliced and stained with TTC.

Data Analysis

The PET images were reconstructed using the Fourier rebinning-filtered back projection method with an attenuation correction, calibrated by the crosscalibration factor. The *CBV* image was calculated using PET data averaged for the last 2 minutes of the 3-minute C^{15}O-HbV scan because the time–activity curve of the brain achieved a plateau at about 1 minute after the tracer administration. The radioactivity concentration of the arterial blood sampled every 1 minute after the C^{15}O-HbV injection was averaged and used for the *CBV* calculation. The *CBF* was calculated from $H_2^{15}O$ images using the steady-state method as reported previously (Kobayashi *et al*, 2011). The average image of the last 3 minutes data of the 5-minute $H_2^{15}O$-PET scan was used for the *CBF* calculation.

Since the radioactivity concentrations of the brain and arterial blood reached a plateau about 2 minutes after $^{15}O_2$-HbV administration (see Results), the average of the last 3 minutes data of the 5-minute $^{15}O_2$-HbV scan were used for *OEF* and $CMRO_2$ calculations. The *OEF* image was calculated from the averaged images of $H_2^{15}O$ and $^{15}O_2$-HbV scans based on the established steady-state method with the following equations (Frackowiak *et al*, 1980; Lammertsma *et al*, 1982);

$$OEF' = \frac{\frac{C_{bO2}}{C_{bH2O}} \cdot \frac{C_{aH2O}}{C_{pO2}} - \frac{C_{aH2O}}{C_{pH2O}}}{\frac{C_{aO2}}{C_{pO2}} - \frac{C_{aH2O}}{C_{pH2O}}} \quad (2)$$

$$C_{aH2O}/C_{pH2O} = 1 - 0.245Ht_a \quad (3)$$

where *OEF*′ is uncorrected *OEF*, C_{bO2}, and C_{bH2O} (Bq/mL) are the average brain radioactivity concentration of the $^{15}O_2$ and $H_2^{15}O$ images. C_{aO2}, C_{pO2}, C_{aH2O}, and C_{pH2O} (Bq/mL) are the mean arterial and plasma concentrations in the $^{15}O_2$ and $H_2^{15}O$ scans, respectively. Ht_a is arterial hematocrit. The *CBV* correction method was applied to the calculation of *OEF* from *OEF*′ as follows (Lammertsma *et al*, 1983; Lammertsma and Jones, 1983).

$$OEF = \frac{OEF' - \frac{CBF/100+\lambda}{CBF/CBV+\lambda}}{1 - \frac{CBF/100+\lambda}{CBF/CBV+\lambda}} \quad (4)$$

In the equation (4), λ is the decay constant of ^{15}O. The $CMRO_2$ was calculated by the following equation using the *CBF*, *OEF* images, and arterial O_2 content (O_2c), which was obtained from the blood gas and hemoglobin data of each rat.

$$CMRO_2 = OEF \times CBF \times O_2c \quad (5)$$

The parametric PET images of normal rats were coregistered with each MRI image using Dr View software (AJS, Tokyo, Japan). In the analysis of normal rats, MRI coronal slices were used to draw ROIs (regions of interest) at three slice levels of the whole brain, frontal cortex, visual cortex, striatum, thalamus, and sensorimotor cortex referring to the rat brain atlas (Kobayashi *et al*, 2011). The same ROIs were applied to all parametric PET images to obtain cerebral hemodynamic parameters in each normal rat. In the MCAO model rats, multiple circle ROIs (2.4 mm in diameter) were placed on the infarction area and the corresponding contralateral regions with reference to the TTC staining brain slices, as well as the MRI images in the three MCAO model rats. The hemodynamic parameters of the affected cortex in the MCAO model rats were compared with the corresponding contralateral region and those of the sensorimotor cortex in the normal rats using one-way analysis of variance with a *post hoc* Sheffe's *F*-test. Blood gas data in the normal and MCAO model rats were also compared using repeated-measures analysis of variance and a *post hoc* paired *t*-test. A P value of <0.05 was considered statistically significant.

Results

Labeling Efficiency and Physiological Parameters

Labeling efficiency values of $H_2^{15}O$, C^{15}O-HbV, and $^{15}O_2$-HbV were 123.4 ± 3.4, 65.7 ± 12.2, and 95.7 ± 4.1 MBq/mL, respectively.

Table 1 shows arterial blood gas data after the transmission scan, and before and after the $^{15}O_2$-HbV PET in the normal and MCAO model rats. Only P_{CO2} values of the MCAO model rats decreased significantly for all conditions compared with normal rats ($P<0.05$), although no rat group showed any difference among conditions (repeated-measures analysis of variance). The injection volume of the $^{15}O_2$-HbV and $H_2^{15}O$ was 1.65 mL during the 5-minute PET scan. The sampled blood volumes were about 0.65 and 1.40 mL for the $H_2^{15}O$ and $^{15}O_2$-HbV scans, respectively.

Normal Rat Study

The $^{15}O_2$-HbV radioactivity concentration rapidly achieved equilibrium in the whole blood, plasma, and the brain at about 2 minutes after radiotracer administration using the same injection program as the $H_2^{15}O$-PET (Figure 1), and the curves were similar to those of $H_2^{15}O$. Representative PET images of a normal rat are given in Figure 2. Table 2 shows hemodynamic parameters of the whole brain mean and the regional cerebral values in the normal rats. The parameters were not significantly different among the brain regions.

Middle Cerebral Arterial Occlusion Model Rat Study

The MCAO model rats also showed rapid radioactivity equilibrium of $H_2^{15}O$ and $^{15}O_2$-HbV in the brain and blood within 2 minutes using the steady-state method. Figure 3 shows MRI images, TTC staining, and ^{15}O-PET images in a MCAO model rat. The TTC staining brain slice revealed an infarction area in the left cerebral hemisphere after MCAO. Cerebral hemodynamic parameters of the

Table 1 Arterial blood gas data in normal and MCAO model rats

	After transmission		*Before $^{15}O_2$-HbV*		*After $^{15}O_2$-HbV*	
	Normal	*MCAO*	*Normal*	*MCAO*	*Normal*	*MCAO*
pH	7.31 ± 0.04	7.31 ± 0.03	7.32 ± 0.06	7.32 ± 0.06	7.32 ± 0.05	7.32 ± 0.06
P_{CO2} (mm Hg)	47.8 ± 2.2	44.0 ± 2.6*	48.6 ± 1.5	39.9 ± 3.8*	49.0 ± 1.1	42.2 ± 3.7*
P_{O2} (mm Hg)	88.2 ± 4.0	87.0 ± 6.0	88.1 ± 5.8	88.0 ± 5.6	90.5 ± 6.5	87.1 ± 7.9
Hct (%)	48.0 ± 2.3	49.2 ± 2.0	47.3 ± 2.3	49.5 ± 1.8	47.3 ± 2.0	48.3 ± 1.7
O_2 Sat (%)	96.7 ± 1.2	95.8 ± 2.3	95.4 ± 2.1	94.7 ± 2.3	97.0 ± 1.3	94.9 ± 3.9
Hb (g/dL)	15.1 ± 0.5	15.5 ± 0.8	15.1 ± 0.4	15.5 ± 0.6	15.1 ± 0.6	15.6 ± 0.6
O_2c (mLO_2/g)	0.20 ± 0.01	0.21 ± 0.01	0.20 ± 0.01	0.21 ± 0.01	0.20 ± 0.01	0.21 ± 0.01

ANOVA, analysis of variance; Hb, hemoglobin; Hct, hematocrit; MCAO, middle cerebral arterial occlusion; O_2 Sat, arterial oxygen saturation; O_2c, O_2 content; P_{CO2}, arterial carbon dioxide tension; P_{O2}, arterial oxygen tension.
*$P < 0.05$ compared between normal rats and MCAO rats for each condition by ANOVA. The three different conditions did not affect blood gas data in any group (repeated-measures ANOVA).

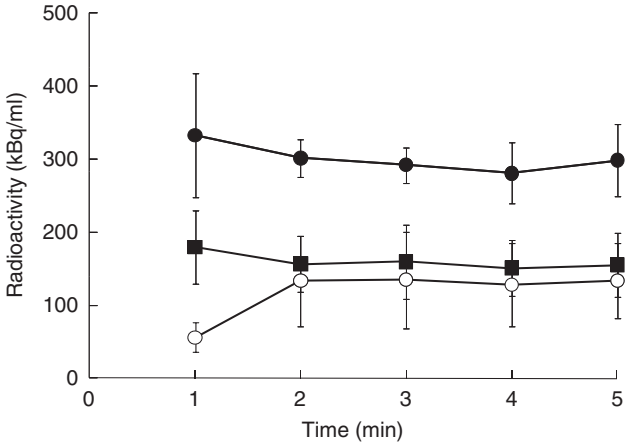

Figure 1 Time–activity curves of the whole blood, plasma, and the whole brain using $^{15}O_2$-HbV with the steady-state method. The radioactivity reached equilibrium in the whole blood (●), plasma, (■) and the whole brain (○) rapidly at ~2 minutes after administration. HbV, hemoglobin-containing vesicles.

normal rats and the MCAO model rats are given in Table 3. The hemodynamic parameters in the contralateral side were not significantly different from those in the sensorimotor cortex of the normal rats. All hemodynamic parameters in the ipsilateral hemisphere decreased significantly compared with the contralateral side ($P < 0.01$).

Discussion

In this study, the steady-state method was applied to $^{15}O_2$-HbV PET to measure the cerebral oxygen metabolism of rats under normal and MCAO conditions, providing rapid radioactivity equilibrium in both the blood and the brain. The physical condition of rats was stable during PET experiments because of the small volumes of injection as well as arterial blood samplings. Injectable $^{15}O_2$-HbV is ideal for measuring the cerebral oxygen metabolism with small animals because $^{15}O_2$-gas inhalation affects cerebral PET counts due to its high nasal radioactivity. Although cerebral oxygen metabolism of normal rats was estimated using the $^{15}O_2$-HbV with a single bolus injection method (Tiwari *et al*, 2010), a small animal may be stressed from frequent multipoint arterial blood samplings in each ^{15}O experiment. In our previous study, the steady-state method was applied to measure *CBF* using $H_2^{15}O$ and provided stable values. The method was considered suitable for repeated *CBF* measurements because it requires only a few arterial blood samplings during the steady state of the PET scan (Kobayashi *et al*, 2011).

The same injection program was applied to $^{15}O_2$-HbV administration in the present study. Although the labeling efficiency of the ^{15}O-radiotracers was slightly different between $H_2^{15}O$ and $^{15}O_2$-HbV (123.4 and 95.7 MBq/mL), the difference did not affect the time to achieve equilibrium of radioactivity in the blood and the brain because the same level of radioactivity of 61.7 MBq/mL for both radiotracers (185 MBq in 3 mL volume) was injected at the scan start. The injection volume of the ^{15}O-radiotracer did not affect the physical condition of the rats during the PET experiments (Table 1) because of the small injection volume (1.0 and 0.25 mL net injection volumes for $H_2^{15}O$ and $^{15}O_2$-HbV, respectively, after subtraction of the sampled blood volumes) and slowly increasing injection velocity (Morton *et al*, 1997). In addition, HbV injection did not change the rats' physical condition. Although the P_{CO2} values in the MCAO model rats were significantly decreased compared with those in the normal rats, probably due to hyperventilation in a few rats during PET experiments, the *CBF* was not affected significantly because other blood gas data were not changed compared with those of normal rats. This effect of MCAO operation on the arterial blood gas data was similar to a previous report (Temma *et al*, 2006). The P_{CO2} values seem slightly higher and the P_{O2} values seem slightly lower in normal rats compared with those in humans probably due to the tendency of hypoventilation under anesthesia during

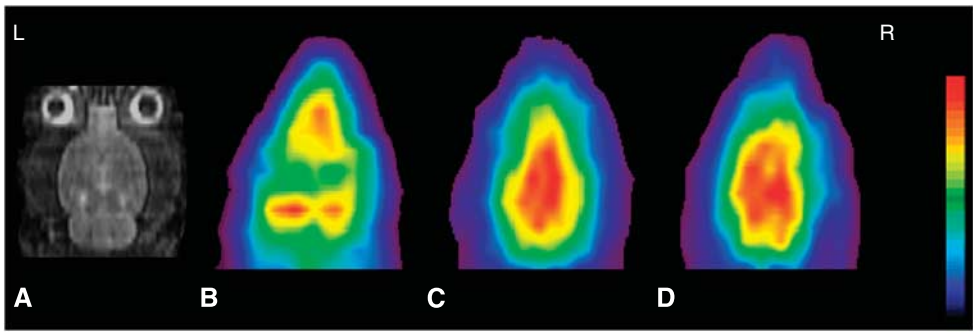

Figure 2 Coronal magnetic resonance imaging (MRI) (**A**), C^{15}O-HbV (**B**), $H_2^{15}O$ (**C**), and $^{15}O_2$-HbV (**D**) positron emission tomography (PET) images of a normal rat. Average PET images of 2 minutes for C^{15}O-HbV, and 3 minutes for $H_2^{15}O$ and $^{15}O_2$-HbV after reaching equilibrium were used to calculate the hemodynamic parameters. Each PET image was coregistered to the individual MRI, and sliced at the same level. The upper values for the color scale were 50, 300, and 300 (kBq/mL) for (**B**), (**C**), and (**D**), respectively. HbV, hemoglobin-containing vesicles.

Table 2 Hemodynamic parameters of normal rats

	Whole brain	*Frontal cortex*	*Visual cortex*	*Striatum*	*Thalamus*
CBF (mL per minute 100 g)	54.3 ± 2.0	54.1 ± 1.8	53.8 ± 2.1	55.1 ± 2.2	56.2 ± 1.8
OEF	0.56 ± 0.04	0.53 ± 0.05	0.56 ± 0.05	0.55 ± 0.04	0.56 ± 0.05
CMRO$_2$ (μmoL per minute per g) (mL per minute per 100 g)	2.78 ± 0.19 (6.2 ± 0.4)	2.60 ± 0.21 (5.8 ± 0.5)	2.73 ± 0.20 (6.1 ± 0.4)	2.72 ± 0.19 (6.1 ± 0.4)	2.82 ± 0.21 (6.3 ± 0.5)
CBV (mL/100 g)	4.9 ± 0.4	5.1 ± 0.5	5.1 ± 0.4	4.8 ± 0.4	5.0 ± 0.5

CBF, cerebral blood flow; CBV, cerebral blood volume; CMRO$_2$, cerebral metabolic rate for oxygen; OEF, oxygen extraction fraction.
See values for the sensorimotor cortex in Table 3.

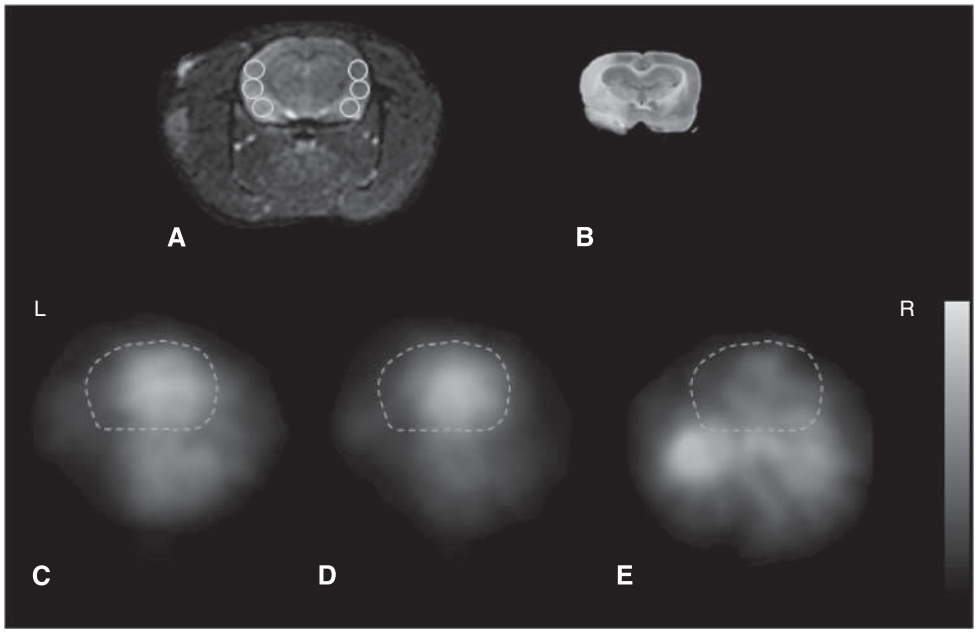

Figure 3 Transaxial magnetic resonance imaging (MRI) (**A**), 2,3,5-triphenyl-tetrazolium chloride (TTC) staining (**B**), $H_2^{15}O$ (**C**), $^{15}O_2$-HbV (**D**), and C^{15}O-HbV (**E**), positron emission tomography (PET) images on a left middle cerebral arterial occlusion (MCAO) model rat. All images are shown at the same slice level, including the sensorimotor cortex, etc. The regions of interest (ROIs) were placed on the infarction in the ipsilateral side and on the normal cortex in the contralateral side (**A**). Dashed lines are contours of the brain. The upper values for the gray scale were 300, 300, and 50 (kBq/mL) for (**C**), (**D**), and (**E**), respectively. HbV, hemoglobin-containing vesicles.

Table 3 Hemodynamic parameters of the rats under normal and MCAO conditions

	Normal (n = *20*)	*MCAO* (n = *10*)	
	Sensorimotor cortex	*Contralateral*	*Ipsilateral*
CBF (mL per minute per 100 g)	55.8 ± 1.8	56.2 ± 1.9	23.8 ± 2.6*
OEF	0.56 ± 0.04	0.54 ± 0.03	0.24 ± 0.04*
CMRO$_2$ (μmol per minute per g) (mL per minute per 100 g)	2.86 ± 0.21 (6.4 ± 0.5)	2.88 ± 0.19 (6.4 ± 0.4)	0.55 ± 0.13* (1.2 ± 0.3*)
CBV (mL/100 g)	5.0 ± 0.4	5.3 ± 1.0	2.8 ± 0.5*

ANOVA, analysis of variance; CBF, cerebral blood flow; CBV, cerebral blood volume; CMRO$_2$, cerebral metabolic rate for oxygen; MCAO, middle cerebral artery occlusion; OEF, oxygen extraction fraction.
*$P < 0.0001$ compared among the three groups (20 hemispheres of normal rats and 10 of contra- and ipsi-lateral hemispheres of MCAO rats) for each hemodynamic parameter using ANOVA and *post hoc* Sheffe's *F*-test.

experiments. Similar results were observed in a previous study with normal rats (Tiwari *et al*, 2010).

In the present study, *OEF* images were corrected using *CBV* images obtained from the C^{15}O-HbV, providing accurate cerebral oxygen metabolism. This blood volume correction has never been applied in small animal studies. The *CBV* correction is necessary because the *CBV* is usually changed in the affected area of a CVD model animal. The *CBV* images were obtained using data from 1 to 3 minutes after C^{15}O-HbV administration because cerebral counts reached a constant level at about 1 minute after administration. The hemodynamic parameters in the contralateral side of the MCAO model rats were not different from those in the normal rats. However, the parameters of the ipsilateral infarction area showed significant decreases (Table 3), because the MCAO model in the present study caused complete infarction in the brain territory of the occluded MCA. Since complete occlusion and infarction would prevent the ability of the tracers to reach the lesion, the MCAO model in this study may affect the time to achieve equilibrium and oxygen membrane permeability in the ischemic tissue, which may influence on quantitative values obtained by the steady-state method. This significant reduction of parameters in the region of cerebral infarction was similar to a previous report (Temma *et al*, 2006). A single-compartment analysis used in the steady-state method may overestimate cerebral water clearance and tissue counts (Ohta *et al*, 1992, 1996); however, this method was established in human PET studies and many studies with CVD patients were reported (Yamauchi *et al*, 1996, 1998, 1999; Okazawa *et al*, 2001; Ouchi *et al*, 2001). Although slightly different values were observed between the steady-state method and the bolus administration method in a previous study with CVD, the values were not significantly different (Okazawa *et al*, 2001).

The $^{15}O_2$-HbV injection yields metabolic ^{15}O-water, which may affect arterial blood and cerebral PET counts. However, the radioactivity of the metabolic water was considered to reach equilibrium in the early phase after $^{15}O_2$-HbV administration because the plasma radioactivity in the $^{15}O_2$-HbV scan reached a plateau at 2 minutes after administration in the present study using the steady-state method (Figure 1). The cerebral radioactivity of $H_2^{15}O$-PET also achieved equilibrium at 2 minutes after administration as reported previously. The average images of $H_2^{15}O$ and $^{15}O_2$-HbV were obtained using PET data from 2 to 5 minutes after administration because cerebral PET counts and arterial blood radioactivity were constant during that time. Stable hemodynamic parameters were obtained with the same quality and noiseless PET images, as well as stable radioactivity of the arterial blood and plasma (Table 2). Although the steady-state method may induce systemic underestimation of *CBF* because of tissue heterogeneity between gray and white matter as compared with the bolus injection method in the human study (Kanno *et al*, 1984); however, the structure of the brain cortex in rats is not so complicated (Zilles and Wree, 1995), and the effect of brain tissue heterogeneity is not considered so significant as compared with the human brain because we placed ROIs on the cortices (Figure 3A) and basal ganglia. The cerebral hemodynamic parameters of the normal rats using the present steady-state method were similar to the results reported previously using the bolus method (Magata *et al*, 2003; Temma *et al*, 2006; Tiwari *et al*, 2010), in which slightly higher values of *OEF* and *CMRO*$_2$ in normal rats were observed compared with those of normal human subjects. Differences in species and effects of anesthesia during the experiments are considered to provide these differences. Higher *CBV* values may also be caused by anesthesia, and many previous reports showed various rage of *CBV* from 2.5 to 4.7 mL/100 g (Sandor *et al*, 1986; Todd *et al*, 1993; Perles-Barbacaru and Lahrech, 2007). A smaller size of HbV than normal RBC may also have affected the *CBV* value because smaller vessels might be delineated by C^{15}O-HbV. The blood pool correction using *CBV* was applied in this steady-state method, and thus, the influence of slightly greater vascular radioactivity on *OEF* values would be negligible.

A small amount of $^{15}O_2$-gas may be detached from $^{15}O_2$-HbV in the lungs and exhaled, which may affect radioactivity in the head and airways of rats during PET scans. However, it has already been reported that the $^{15}O_2$-gas released from the nose and mouth showed little influence on quantitative values of cerebral oxygen metabolism in previous studies using injectable $^{15}O_2$ (Magata *et al*, 2003; Temma *et al*, 2006). Although the radioactivity of $^{15}O_2$ released from the nose and mouth of the rats in $^{15}O_2$-HbV studies has never been measured, the influence of detached $^{15}O_2$ on quantitative hemodynamic values would be similarly small, as in previous studies. The penumbra regions were not examined in this study because a reperfusion model after MCAO was not applied and most of the ischemic regions showed infarction. A reperfusion model after MCAO would be appropriate to evaluate the pathophysiology of the penumbra area. In the rats with MRI images, the brains were excluded about 15 to 20 minutes after the PET scans. There was a slight time difference from the procedure without MRI in the timing of the TTC staining; however, the infarction area in the TTC staining was not significantly different from that in the PET and MRI images (Figure 3).

In conclusion, $^{15}O_2$-HbV with the steady-state method is stable and useful, and may be ideal to measure the cerebral oxygen metabolism of small animals with less stress. The *CBV* correction with C^{15}O-HbV provides precise cerebral oxygen metabolism, especially in CVD model animals. Basic research with CVD models will be accelerated by injectable ^{15}O-HbV tracers with the steady-state method.

Acknowledgements

The author thanks Satonao Nakakoji, Akira Ito, Hiroshi Oikawa, and other staff of the Biological Imaging Research Center, University of Fukui for their technical support.

Disclosure/conflict of interest

The authors declare no conflict of interest.

References

Frackowiak RS, Lenzi GL, Jones T, Heather JD (1980) Quantitative measurement of regional cerebral blood flow and oxygen metabolism in man using ^{15}O and positron emission tomography: theory, procedure, and normal values. *J Comput Assist Tomogr* 4:727–36

Kanno I, Lammertsma AA, Heather JD, Gribbs JM, Rhodes CG, Clark JC, Jones T (1984) Measurement of cerebral blood flow using bolus inhalation of C$^{15}O_2$ and positron emission tomography: description of the method and its comparison with the C$^{15}O_2$ continuous inhalation method. *J Cereb Blood Flow Metab* 4:224–34

Kobayashi M, Kiyono Y, Maruyama R, Mori T, Kawai K, Okazawa H (2011) Development of an $H_2^{15}O$ steady-state method combining a bolus and slow increasing injection with a multiprogramming syringe pump. *J Cereb Blood Flow Metab* 31:527–34

Kuge Y, Minematsu K, Yamaguchi T, Miyake Y (1995) Nylon monofilament for intraluminal middle cerebral artery occlusion in rats. *Stroke* 26:1655–7

Lammertsma AA, Heather JD, Jones T, Frackowiak RS, Lenzi GL (1982) A statistical study of the steady state technique for measuring regional cerebral blood flow and oxygen utilisation using ^{15}O. *J Comput Assist Tomogr* 6:566–73

Lammertsma AA, Jones T (1983) Correction for the presence of intravascular oxygen-15 in the steady-state technique for measuring regional oxygen extraction ratio in the brain: 1. Description of the method. *J Cereb Blood Flow Metab* 3:416–24

Lammertsma AA, Wise RJ, Heather JD, Gibbs JM, Leenders KL, Frackowiak RS, Rhodes CG, Jones T (1983) Correction for the presence of intravascular oxygen-15 in the steady-state technique for measuring regional oxygen extraction ratio in the brain: 2. Results in normal subjects and brain tumour and stroke patients. *J Cereb Blood Flow Metab* 3: 425–31

Longa EZ, Weinstein PR, Carlson S, Cummins R (1989) Reversible middle cerebral artery occlusion without craniectomy in rats. *Stroke* 20:84–91

Magata Y, Temma T, Iida H, Ogawa M, Mukai T, Iida Y, Morimoto T, Konishi J, Saji H (2003) Development of injectable O-15 oxygen and estimation of rat OEF. *J Cereb Blood Flow Metab* 23:671–6

Morton D, Safron JA, Rice DW, Wilson DM, White RD (1997) Effects of infusion rates in rats receiving repeated large volumes of saline solution intravenously. *Lab Anim Sci* 47:656–9

Ogata Y (2000) Characteristics and function of human hemoglobin vesicles as an oxygen carrier. *Polym Adv Technol* 11:205–9

Ohta S, Meyer E, Thompson CJ, Gjedde A (1992) Oxygen consumption of the living human brain measured after a single inhalation of positron emitting oxygen. *J Cereb Blood Flow Metab* 12:179–92

Ohta S, Meyer E, Fujita H, Reutens DC, Evans A, Gjedde A (1996) Cerebral water clearance in humans determined by PET: I. Theory and normal values. *J Cereb Blood Flow Metab* 16:765–80

Okazawa H, Yamauchi H, Sugimoto K, Takahashi M, Toyoda H, Kishibe Y, Shio H (2001) Quantitative comparison of the bolus and steady-state methods for measurement of cerebral perfusion and oxygen metabolism: PET study using ^{15}O-gas and water. *J Cereb Blood Flow Metab* 21:793–803

Ouchi Y, Nobezawa S, Yoshikawa E, Futatsubashi M, Kanno T, Okada H, Torizuka T, Nakayama T, Tanaka K (2001) Postural effects on brain hemodynamics in unilateral cerebral artery occlusive disease: a positron emission tomography study. *J Cereb Blood Flow Metab* 21:1058–66

Perles-Barbacaru AT, Lahrech H (2007) A new magnetic resonance imaging method for mapping the cerebral blood volume fraction: the rapid steady-state T1 method *J Cereb. Blood Flow Metab* 27:618–31

Phillips WT, Lemen L, Goins B, Rudolph AS, Klipper R, Fresne D, Jerabek PA, Emch ME, Martin C, Fox PT, McMahan CA (1997) Use of oxygen-15 to measure

oxygen-carrying capacity of blood substitutes *in vivo*. *Am J Physiol* 272:2492–9

Sandor P, Put JC, de Jong W, de Wied D (1986) Continuous measurement of cerebral blood volume in rats with the photoelectric technique: effect of morphine and naloxone. *Life Sci* 39:1657–65

Takeoka S, Teramura Y, Atoji T, Tsuchida E (2002) Effect of Hb-encapsulation with vesicles on H2O2 reaction and lipid peroxidation. *Bioconjug Chem* 13:1302–8

Temma T, Magata Y, Kuge Y, Shimonaka S, Sano K, Katada Y, Kawashima H, Mukai T, Watabe H, Iida H, Saji H (2006) Estimation of oxygen metabolism in a rat model of permanent ischemia using positron emission tomography with injectable ^{15}O-O_2. *J Cereb Blood Flow Metab* 26:1577–83

Temma T, Kuge Y, Sano K, Kamihashi J, Obokata N, Kawashima H, Magata Y, Saji H (2008) PET O-15 cerebral blood flow and metabolism after acute stroke in spontaneously hypertensive rats. *Brain Res* 1212:18–24

Tiwari VN, Kiyono Y, Kobayashi M, Mori T, Kudo T, Okazawa H, Fujibayashi Y (2010) Automatic labeling method for injectable ^{15}O-oxygen using hemoglobin-containing liposome vesicles and its application for measurement of brain oxygen consumption by PET. *Nucl Med Biol* 37:77–83

Todd MM, Weeks JB, Warner DS (1993) Microwave fixation for the determination of cerebral blood volume in rats. *J Cereb Blood Flow Metab* 13:328–36

Yamada R, Watanabe M, Omura T, Sato N, Shimizu K, Takahashi M, Ote K, Katabe A, Moriya T, Sakai K, Yamashita T, Tanaka E (2008) Development of a small animal PET scanner using DOI detectors. *IEEE Trans Nucl Sci* 55:906–11

Yamauchi H, Fukuyama H, Nagahama Y, Nabatame H, Nakamura K, Yamamoto Y, Yonekura Y, Konishi J, Kimura J (1996) Evidence of misery perfusion and risk for recurrent stroke in major cerebral arterial occlusive diseases from PET. *J Neurol Neurosurg Psychiatry* 61:18–25

Yamauchi H, Fukuyama H, Nagahama Y, Katsumi Y, Okazawa H (1998) Cerebral hematocrit decreases with hemodynamic compromise in carotid artery occlusion. A PET study. *Stroke* 29:98–103

Yamauchi H, Fukuyama H, Nagahama Y, Nabatame H, Ueno M, Nishizawa S, Konishi J, Shio H (1999) Significance of increased oxygen extraction fraction in 5-year prognosis of major cerebral arterial occlusive diseases. *J Nucl Med* 40:1992–8

Zilles K, Wree A (1995) Cortex: areal and laminar structure. In: *The Rat Nervous System* (Paxinos G, eds), 2nd ed, San Diego, CA: Academic Press, Inc., 649–85